

AIAA-94-301 o

Experimental Evaluation of Russian Anode Layer Thrusters

Charles E. Garner, James E. Polk, John R. Brophy, and Colleen Marrese

*Jet Propulsion Laboratory
California Institute of Technology
Pasadena, California*

Sasha Semenkin, Sergey Tverdokhlebov
*Central Research Institute of Machine Building
Kaliningrad (Moscow Region), Russia*

Performance and endurance testing of a 1.35 kW thruster with anode layer (TAL), developed at the Central Research Institute of Machine Building (TsNIIMASH) is described. The TAL evaluated herein is designated the D-55 and is characterized by an external accelerator in ozone to maximize engine life. Performance measurements indicate that the D-55 performance is comparable to that of the SPT-100 for operation at 1.35 kW. A 687 hour accelerated wear test was performed to assess the thruster service life capability. For this test the TsNIIMASH cathode was replaced by a cathode fabricated at JPL to eliminate concerns over cathode durability since the primary objective of the test was to evaluate the discharge chamber erosion characteristics. Post test examination indicated that the volume of material removed over the course of the wear test was a factor of XX less than for the SPT-100 over the same operation duration. Most of the erosion takes place on guard rings which protect the magnetic circuit pole pieces from erosion. Changing this ring material from stainless steel to a more sputter-resistant material, such as graphite, will further reduce the erosion rate and yield engine life times estimated to be greater than 5,000 hours.

Introduction

Hall thrusters have generated a great deal of interest world-wide since the introduction of the Russian stationary plasma thruster, SPT-100, to the West at the beginning of this decade. Performance evaluations^{1,2} and on-going endurance tests^{3,4} continue to support claims that the SPT-100 thruster is a robust device with excellent operating characteristics. A different type of Hall thruster, the thruster with anode layer (TAL), also developed in Russia, has performance characteristics which are comparable to those of the stationary plasma thrusters. For the same power level, however, the TAL discharge chamber is physically smaller than that of the SPT. The D-55 TAL, for example, has a nominal operating power level of 1.35 kW and a characteristic discharge chamber diameter of only 55 mm or almost half of the characteristic dimension of the 100 mm diameter 1.35-kW, SPT-100. Never-the-less, in spite of the increased thrust density

corresponding to its small physical size, there is reason to believe that the TAL with "external layer" may have erosion characteristics superior to the SPT.

For this reason, the Ballistic Missile Defense Organization (BMDO) has sponsored a program to evaluate the performance, erosion characteristics and integration issues associated with the anode layer thruster.⁶ The program is being executed primarily by NASA Lewis Research Center (LeRC) and the Jet Propulsion Laboratory (JPL) in cooperation with the Central Research Institute for Machine Building (TsNIIMASH) in Kaliningrad (Moscow region), Russia. Performance testing and evaluation of integration issues are being performed at LeRC⁷, while performance and endurance testing is being done at JPL. Two types of anode layer thrusters were purchased from TsNIIMASH, the 1.35 kW D-55 and the 4.5 kW D-100. This paper describes the performance and endurance testing of the D-55 TAL at JPL.

Historical Background

The physical principle of the thruster with anode layer was first proposed by A. V. Zharinov more than 30 years ago.^{8,9,10} Work at TsNIIMASH in the early 1960s under his guidance emphasized understanding the fundamental physics of anode layer thruster operation. Members of Zharinov's team included V. S. Erofeev, M. A. Abdukhanov, and Yu. S. Popov. The TAL research at TsNIIMASH was part of a larger program to investigate a wide variety of plasma accelerators under the supervision of S. D. Grishin.

Early development of the anode layer thruster concentrated on the double-stage configuration.^{11,12} The first stage in this thruster is a low voltage discharge with closed Hall current used for ion generation. In the second stage the ions are accelerated by the electric field of the anode layer produced in a transverse magnetic field. Such engines were designed for application to Solar System exploration spacecraft and have specific impulses ranging from 2,000 to 8,000 s.

By the end of the 1960s a double-stage TAL using bismuth as the propellant had been operated at up to 100 kW with a specific impulse of 8,000 s and a total efficiency of close to 0.8.^{12,13} Wear tests of a few hundred to a thousand hours indicated an engine lifetime of a few thousand hours.¹⁴ Cesium and xenon propellants were also investigated.

By the 1970s, thruster development out paced the availability of high power levels in space and the program was redirected to emphasize the development of low (-1 kW) and medium (-10 kW) power level thrusters operating on rare gases (especially xenon). Research efforts centered on the development of a single-stage anode layer thruster,^{15,16} and also on understanding the thruster dynamic characteristics^{17,18,19} and service life capabilities.^{16,20} The product of this effort was the high efficiency, single-stage anode layer thruster.^{20,21} To achieve long thruster lifetimes one of the principal innovations was the development of the TAL with external layer in which the ion production and ion acceleration regions actually exist just downstream of the exit plane of the thruster. This configuration greatly reduces the flux of energetic ions to thruster surfaces thereby significantly reducing the erosion of those surfaces.

Apparatus and Procedure

D-55 Design and Operation

The single-stage, D-55 TAL, shown in Fig. 1, consists of an annular discharge chamber in which the anode electrode extends nearly to the exit plane of the thruster as suggested in Fig. 2. In a fashion similar to the SPT, a radial magnetic field is established across the annular discharge chamber through the use of electromagnets. The strength of the magnetic field is sufficient to magnetize the electrons but not the ions, Tayloring of the magnetic field is accomplished in part through the use of a two-piece anode. The downstream section of the anode is molybdenum, which is transparent to the magnetic field. The upstream anode section is nickel-cobalt which shunts the magnetic field lines at the upstream end of the discharge chamber. This has the effect of concentrating the magnetic flux density in the region of space just beyond the molybdenum portion of the anode. This in turn establishes the most of the anode to cathode voltage difference in this region, which is roughly half the axial length of that in the SPT-100 thruster.

An external cathode is used to supply electrons to the discharge chamber, as well as neutralize the ion beam. During normal operation most of the applied voltage difference between the anode and the cathode appears in a relatively thin layer adjacent to the anode. In the modern version of the single-stage TAL, this layer exists just downstream of the exit plane of the thruster and the thruster is referred to as a TAL with external layer. By positioning the ionization and acceleration zone downstream of the discharge chamber walls, erosion of the thruster is minimized.

Surrounding the OD of the anode is a guard ring (see Fig. 2) designed to protect the steel magnetic circuit pole piece from ion sputtering. A similar guard ring is positioned inside the ID of the anode. The separation between the guard rings, which are at cathode potential and the anode, is approximately 0.97 mm for the outer ring and 1.14 mm for the inner one. A possible failure mechanism for the thruster is shorting of the anode to the guard ring by a flake of sputter deposited material. In the thruster tested at JPL the guard rings were fabricated from stainless steel. It is recognized that substitution of a more sputter-resistant material, such as graphite, would substantially increase the thruster life. The use of stainless steel in the thruster for the endurance test results in an accelerated erosion test in that the erosion characteristics obtained over a relative short time with stainless steel should be representative of much longer operation with graphite.

The cathode consists of a LaB_6 emitter in tantalum tube. A tungsten heater is used to preheat the cathode prior to starting. A starter electrode positioned adjacent to the cathode is used only during startup. Little effort has been expended at TsNIMASH in the development and optimization of hollow cathodes since this technology already exists at other Russian organizations (Fakel Design Bureau for example, makers of the SPT-100 hollow cathodes).

The D-55 laboratory model thruster also did not come with a flow splitter or flow control hardware, so independent control of the main and cathode flow rates was accomplished manually,

Engine Startup and Operation

startup and operation stuff,.

Test Facility

All testing of the D-55 thruster was performed in a 2.4-m dia. x 5-m stainless steel equipped with oil diffusion pumps to give an effective pumping speed on xenon of approximately 14,000 L/s. A radiation cooled, graphite beam target was positioned at the end of the vacuum chamber opposite the thruster. In addition, the side walls of the chamber were lined in graphite to minimize the rate of material back-sputtered to the thruster.

A laboratory propellant feed system, shown schematically in Fig. 3, was assembled and carefully leaked checked. The micrometer valves controlling the main and cathode flow rates are positioned inside the vacuum chamber. The xenon feed pressure is dropped across the micrometer valves from XX Pa (30 psig) to YY Pa (a few torr) or less for the engine. Since the feed pressure is above atmospheric pressure, this arrangement guarantees that no air can leak into the propellant feed system. Rotary vacuum feedthroughs are used to adjust the micrometer valves from outside the vacuum chamber.

The power supply schematic is shown in Fig. 4. Laboratory power supplies are used for all functions. The main run supply is a 12-kW, custom Spellman high voltage supply. Laboratory power supplies were used for both the cathode tip heater and for the cathode starter. A data acquisition and control system using LabView software and National Instruments hardware was used to record the operating data and permit unattended operation.

Thruster performance was measured using a modified version of the inverted pendulum type thrust stand developed at NASA LeRC.²³ Thrust stand calibrations are performed in situ and under computer control. Generally 40 to 80 calibrations are performed autonomously in order to obtain a large enough sampling for statistical analyses. Repeatability of the calibrations were normally 0.6% or better. During thruster operation, the thrust stand inclination is corrected every 30 s by the computer. To get the most accurate thrust measurements it is necessary to shut off the thruster. The thrust is determined by the difference in thrust stand LVDT signals with the thruster on and off. This approach minimizes any effects due to long term thrust stand zero drifts. In the course of the wear test the thruster was shut off approximately once every 24 hours to get an accurate thrust measurement. This procedure also helped to accumulate on/off cycles on the thruster,

JPL Cathode

Engine performance was measured with two different cathodes, the LaB_6 cathode from TsNIMASH and a cathode fabricated at JPL. The JPL cathode consists of a 6.4-mm diameter molybdenum tube with a barium oxide impregnated porous tungsten insert. A 2% thoriated tungsten orifice plate, with an orifice diameter of 1.3 mm is electron-beam welded to the downstream end. A tantalum-sheathed tantalum heater wire is wrapped around the molybdenum tube to form the tip heater. An "enclosed keeper" starter electrode made of graphite surrounds the cathode. The endurance test was performed with the JPL cathode.

Performance Results

Reason(s) for replacing the TsNIMASH cathode with the JPL cathode
Engine efficiency as a function of input power is given in Fig. 5. These data suggest an engine performance which is comparable to that of the SPT-100 thruster.

Endurance Test

To investigate the erosion characteristics and evaluate the prospects for achieving a useful service life of several thousand hours, a 500 hour wear test at 1.35 kW was planned. At the completion of 500 hours the engine was operating so well that it was decided to

continue the test. A photograph of the D-55 taken during the wear test is shown in Fig. 6. The glowing regions evident in this photograph are believed to be sputter deposits on the anode. The extent of these glowing regions grew steadily over the duration of the wear test. The test was terminated after 687 hours of operation when the thrust stand tilt mechanism failed. Without the ability to accurately measure the thrust it was decided to terminate the test and examine condition of the thruster. The post-test condition of the thruster is shown in Figs. 7 and 8. The erosion of discharge chamber components is difficult to see both in this photograph and on the actual hardware.

Performance History

The thrust, discharge voltage, discharge current, mass flow rate and floating voltage are given in Fig. 9 as a function of time over the wear test. The floating voltage is the potential difference between the cathode and facility ground. The engine/power supply combination is operated ungrounded as indicated in Fig. 3. The data in Fig. 9 indicate essentially no change in the engine performance over the wear test. The scatter in the data over the first 20 hours was due to changes in operating conditions as the thruster performance envelope was explored.

Current and Voltage oscillations

oscillation stuff..

Beam Profiles

Beam profiles were measured using a single Faraday button probe mounted to motorized arm which could swing the probe through an arc 1 m in radius from the thruster. The Faraday probe surface was covered with plasma sprayed tungsten to minimize secondary electron emission effects. A comparison of beam profiles taken at cycles 95 and 128, corresponding to run times of XX hours and 687 hours, is given in Fig. 10. These data indicate essentially no change in the beam shape over the course of the wear test.

Erosion Results

During the 687 hours that the thruster was run, a dark gray material was deposited on the anode. Material analysis by EDAX indicated that the primary

elements of the deposits are the constituents of stainless steel, as well as carbon, molybdenum and xenon. The carbon is most likely backsputtered material from the graphite beam target and the stainless steel is probably from the guard rings. The xenon is obviously trapped propellant and the molybdenum is from the anode and was found only on the side of the deposits adjacent to the anode surface. The deposits were greatest on the anode and barely noticeable on the other thruster components. The maximum thickness of the deposited material was 11 μm . The entire anode appeared to be covered by a layer of this material except for an area of about 242 mm^2 on the back wall of the anode located near the position of the cathode. In this region, the anode seemed to be covered with a thin oxide layer, giving the material a discolored appearance.

Post test inspection of the thruster also revealed a crack in the anode that propagated around the outer circumference a distance of approximately 22.1 mm upstream for the downstream end of the outer guard ring. It is unclear at this time if the crack propagated through to the inner surface of the anode. This crack was not noticed in pre-wear test inspections so it is likely to be a consequence of the thermal cycling which occurred during testing.

Erosion of the inner and outer guard rings was caused by ion sputtering. The erosion depth in the direction parallel to the thruster axis of the inner guard ring is given in Fig. 11 as a function of clock angle (see Fig. 8 for 0° axis reference) for three different radial distances from the thruster axis. The erosion depth typically varies from zero to 0.25 mm, with a maximum measured depth of 0.75 mm.

Similar erosion depth measurements for the outer guard ring are given in Fig. 12 for three radial positions on the ring. These erosion data appear to have a roughly sinusoidal shape with the minimum erosion depths occurring at the clock angles corresponding to the locations of the electromagnets. The maximum measured erosion depth on the outer guard ring was 1.25 mm.

Estimated volume and mass of material removed

Comparison with SPT-100 thruster
Thruster life estimation with material change from ss to graphite

Conclusions

The thruster performance of the D-55 anode layer thruster appears to be comparable to that of the SPT-100. . . .

Acknowledgments

The authors thank Mr. Allison Owens, Mr. Lew Pless, Mr. Robert Toomath and Mr. Keith Goodfellow for their assistance in assembling the experimental support hardware. The work described in this paper was performed by the Jet Propulsion Laboratory, California Institute of Technology, and was supported by the Ballistic Missile Defense Organization through an agreement with the National Aeronautics and Space Administration.

References

- 1 Garner, C. E., Polk, J. E., Pless, L. C., Goodfellow, K. D., and Brophy, J. R., "Performance Evaluation and Life Testing of the SPT-100," IMC-93-091, presented at the 23rd International Electric Propulsion Conference, Seattle, WA, September, 1993.
- 2 Sankovic, J., Hamley, J., and Haag, T., "Performance Evaluation of the Russian SPT-100 Thruster at NASA LeRC," IEPC-93-094, presented at the 23rd International Electric Propulsion Conference, Seattle, WA, September, 1993.
- 3 Garner, C. E., Polk, J. E., and Brophy, J. R., "Cyclic Endurance Test of a SPT-100 Stationary Plasma Thruster," AMA-94-2856, to be presented at the 30th Joint Propulsion Conference, Indianapolis, IN, June 1994.
- 4 Arkhipov, B., et al., "SPT-100 Module Lifetime Test Results," AMA-94-2854, to be presented at the 30th Joint Propulsion Conference, Indianapolis, IN, June 1994.
- 5 Lyapin, E. A., Garkusha, V. I., Seminkin, A. V., and Ivrodokhilev, S. O., "Anode Layer Thrusters: State-of-the-Art and Perspectives," IEPC-93-228, presented at the 23rd International Electric Propulsion Conference, Seattle, WA, September, 1993.
- 6 Cavcny, L., Cut'ran, I., and Brophy, J., "High Performance Electric Propulsion Systems to Meet Mission Opportunities," AMA-94-2736, to be presented at the 30th Joint Propulsion Conference, Indianapolis, IN, June 1994.
- 7 Sankovic, J., Haag, T., and Hamley, J., "Operating Characteristics of the Russian D-55 Anode Layer Thruster," AIM-94-30 11, to be presented at the 30th Joint Propulsion Conference, Indianapolis, IN, June 1994.
- 8 Zharinov, A. V. and Popov, Yu. S., "Acceleration of Plasma by a Closed Hall Current," *Sov. Phys. -- Tech. Phys.*, Vol. 12, pp. 208-211, August 1967.
- 9 Yushmanov, E. E., "Radial Distribution on Potential in the Cylindrical Magnetic Trap for Ion Injection on the Magnetron Type," in *Plasma Physics and the Problem of Controlled Thermonuclear Reactions*, Vol. 4, pp. 235-257, Academy of Sciences of the USSR, Moscow, 1958 (in Russian).
- 10 Grishin, S. D., Yerofeyev, V. S., and Zharinov, A. V., "Accelerators with Closed Hall Current," in *Plasma Accelerators*, L. A. Artsymovich, ed., pp. 54-61, Mashinostroenie, Moscow, 1973 (in Russian).
- 11 Grishin, S. D., Leskov, L. V., and Kozlov, N. I., *Electric Thrusters*, Mashinostroenie, Moscow, 1975 (in Russian).
- 12 Yerofeyev, V. S., Zharinov, A. V., and Lyapin, Ye. A., "Two-Stage Acceleration of Ions in Layer with Closed Hall Currents," in *Plasma Accelerators*, L. A. Artsymovich, ed., pp. 54-61, Mashinostroenie, Moscow, 1973 (in Russian).
- 13 Grishin, S. D., Yerofeyev, V. S., Zharinov, A. V., Naumkin, V. P., and Safronov, I. N., "Characteristics of Two-Stage Ion Accelerators with Anode Layer," *Journal of Applied Mathematics and Technical Physics*, No. 2, pp. 28-36, 1978 (in Russian).
- 14 Grishin, S. D., and Leskov, L. V., *Electric Thrusters of Spacecraft*, Mashinostroenie, Moscow, 1989 (in Russian).
- 15 Yerofeyev, V. S., and Lyapin, Ye. A., "Integral Characteristics of Ion Source of Hall Accelerator with Anode Layer," Abstracts for II All-Union Conference on Plasma Accelerators, pp. J 34-135, Minsk, 1973 (in Russian).
- 16 Lyapin, Ye. A., and Seminkin, A. V., "State-of-the-Art in Investigations of Anode Layer Accelerators," in *Ion Injectors and Plasma Accelerators*, pp. 20-33, Energoizdat, Moscow, 1990 (in Russian).
- 17 Lyapin, Ye. A., and Pelepin, Ye. V., "Ion current Oscillations in Anode Layer Accelerator,"

Plasma Physics, Vol. 5, No. 3, pp. 600-606, 1979 (in Russian).

¹⁹Lyapin, Ye. A., Michailov, K. K., and Podgomova, V. D., "Oscillations in Single-Stage Anode Layer Accelerator," in *Plasma Accelerators and Ion Injectors*, pp. 21-22, Dnepropetrovsk, 1986 (in Russian).

²⁰Lyapin, Ye. A., and Semenkin, A. V., "Accelerator with External Anode Layer," Abstracts for VII All-Union Conference on Plasma Accelerators and Ion Injectors, pp 210-211, Charkov, 1989 (in Russian).

²¹Garkusha, V. I., Leskov, L. V., and Lyapin, Ye. A., "Plasma Accelerators with Anode Layers," in *Plasma Accelerators and Ion Injectors with Anode Layers*, pp. 129-138, Nauka, Moscow, 1984 (in Russian).

²²Semenkin, A. V., "Investigation of Erosion in Anode Layer Thruster and Elaboration High Life Design Scheme," IEPC-93-231, presented at the 23rd International Electric Propulsion Conference, Seattle, WA, September 1993.

²³Haag, T. W. and Curran, F. M., "Arcjet Starting Reliability: A Multistart Test on Hydrogen-Nitrogen Mixtures," AIM-87-106 1, May 1987 (see also NASA TM-898867).

Figure Titles

Fig. 1 Anode layer thruster schematic and pre-test photographs with the JPL cathode,

Fig. 2 Cross section schematic of the D-55.

Fig. 3 Laboratory propellant feed system.

Fig. 4 Power supply system block diagram.

Fig. 5 Engine efficiency and specific impulse vs input power (with JPL cathode).

Fig. 6 Photograph of the D-55 in operation during the wear test.

Fig. 7 Post endurance test condition of the D-55 discharge chamber.

Fig. 8 Details of the D-55 erosion geometry.

Fig. 9 Thrust, specific impulse, discharge voltage, total mass flow rate, and floating voltage during the wear test,

Fig. 10 Comparison of exhaust beam current density profile 1-m downstream of the thruster after XX and 687 hours of operation.

Fig. 11 Erosion depth measurements on the inner guard ring as a function of clock angle and radial distance.

Fig. 12 Erosion depth measurements on the outer guard ring as a function of clock angle and radial distance.

Anode Layer Thruster-55

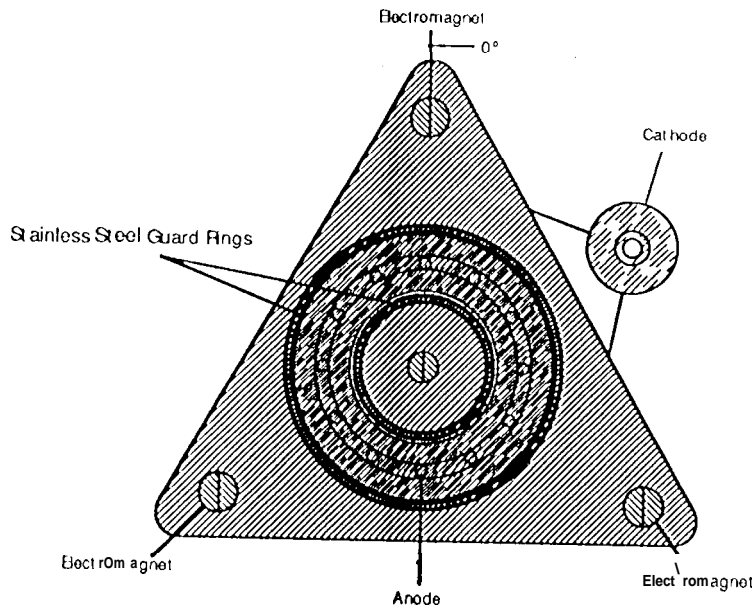


Fig. 1(a). Anode layer Thruster schematic,

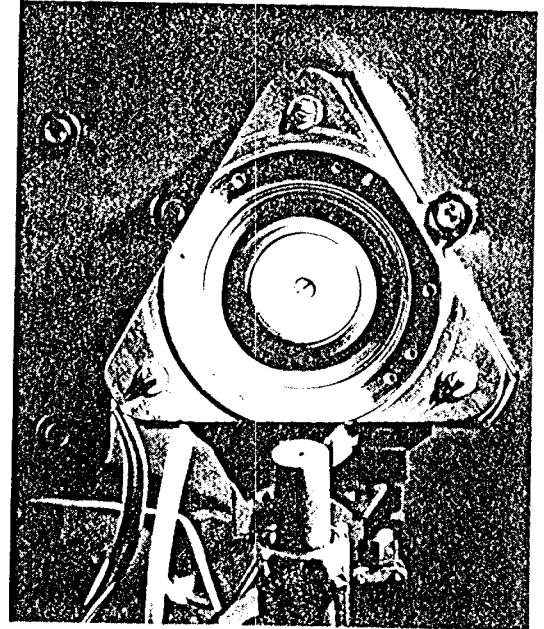


Fig. 1 (b). Pre-test photograph with the JPL cathode

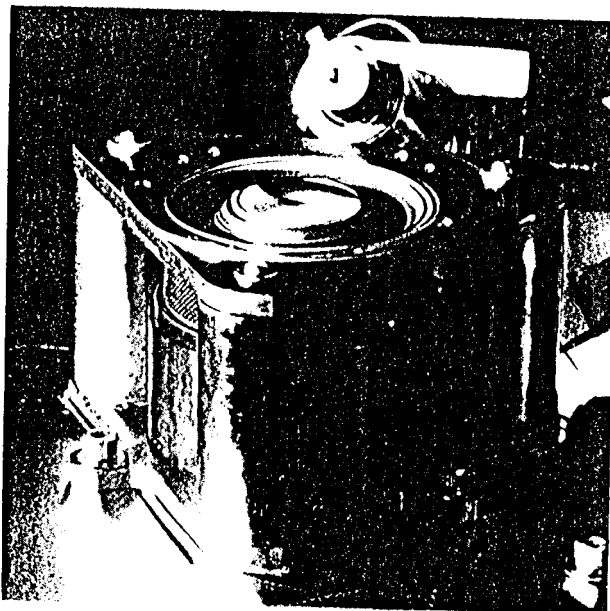


Fig. I (c). Pre-test phonograph with the JPL cathode.

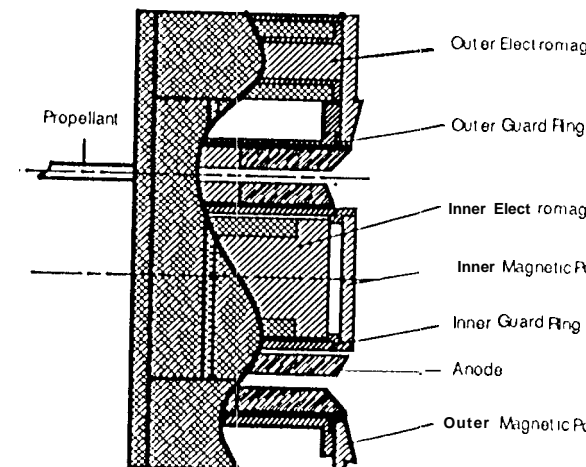


Fig. 2 Cross-section schematic of the D-55.

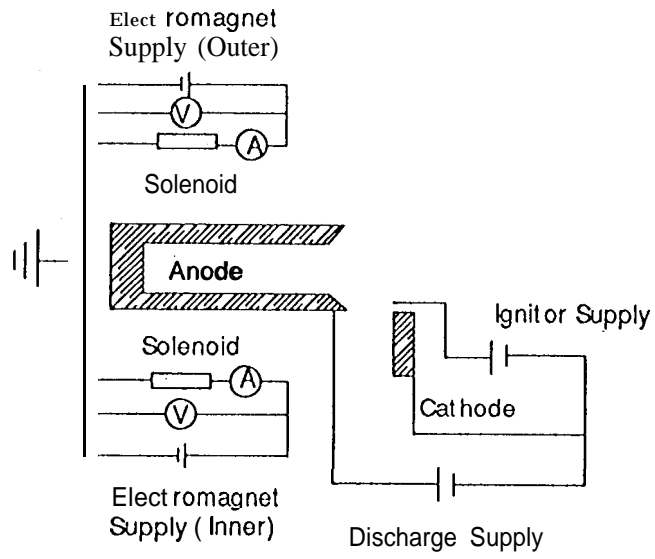


Fig. 3 Power supply system schematic

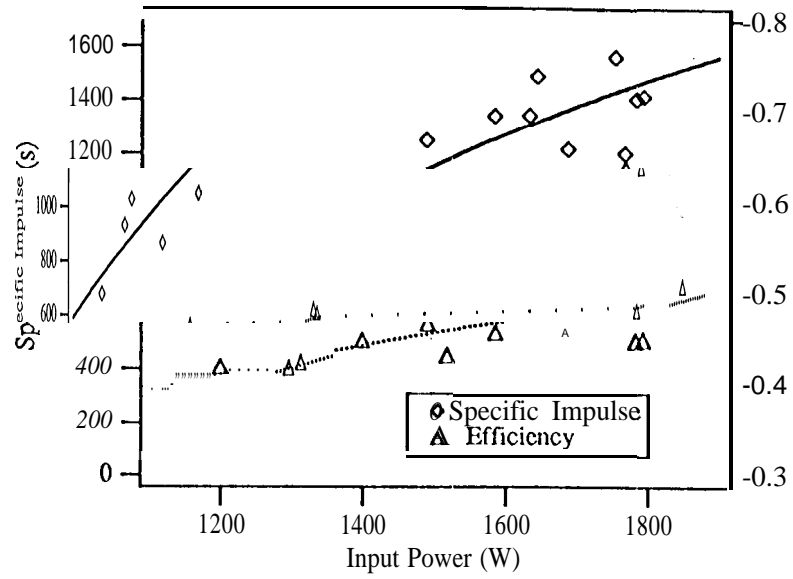


Fig. 4 Specific impulse and engine efficiency vs. input power (with JPL cathode)

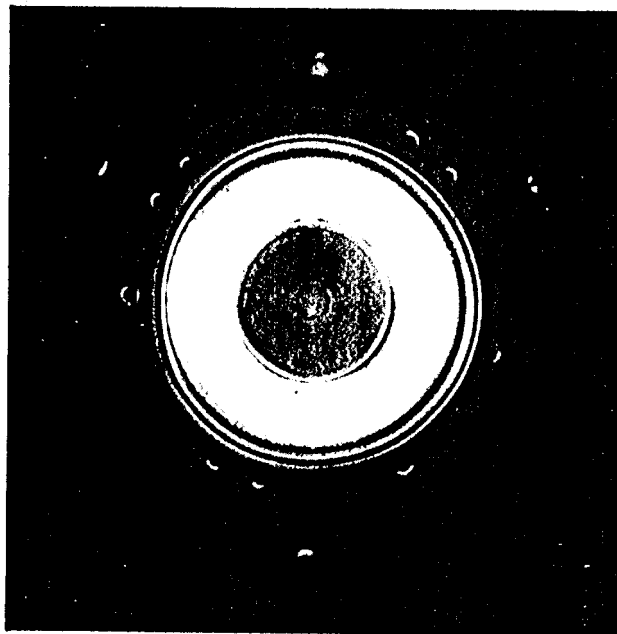


Fig. 5 The D-55 in operation.

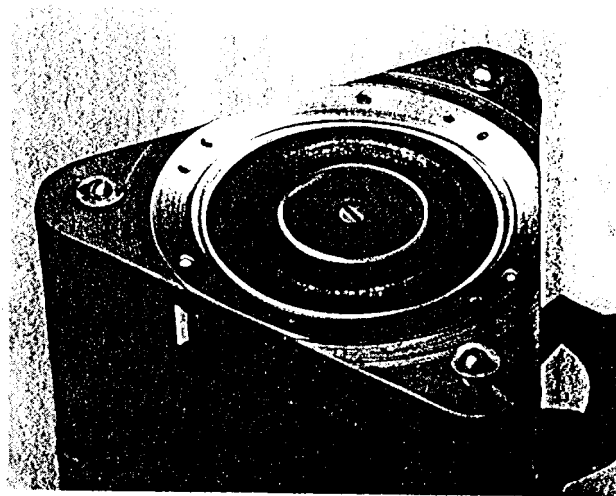


Fig. 6 Post wear test condition of the D-55 discharge chamber.

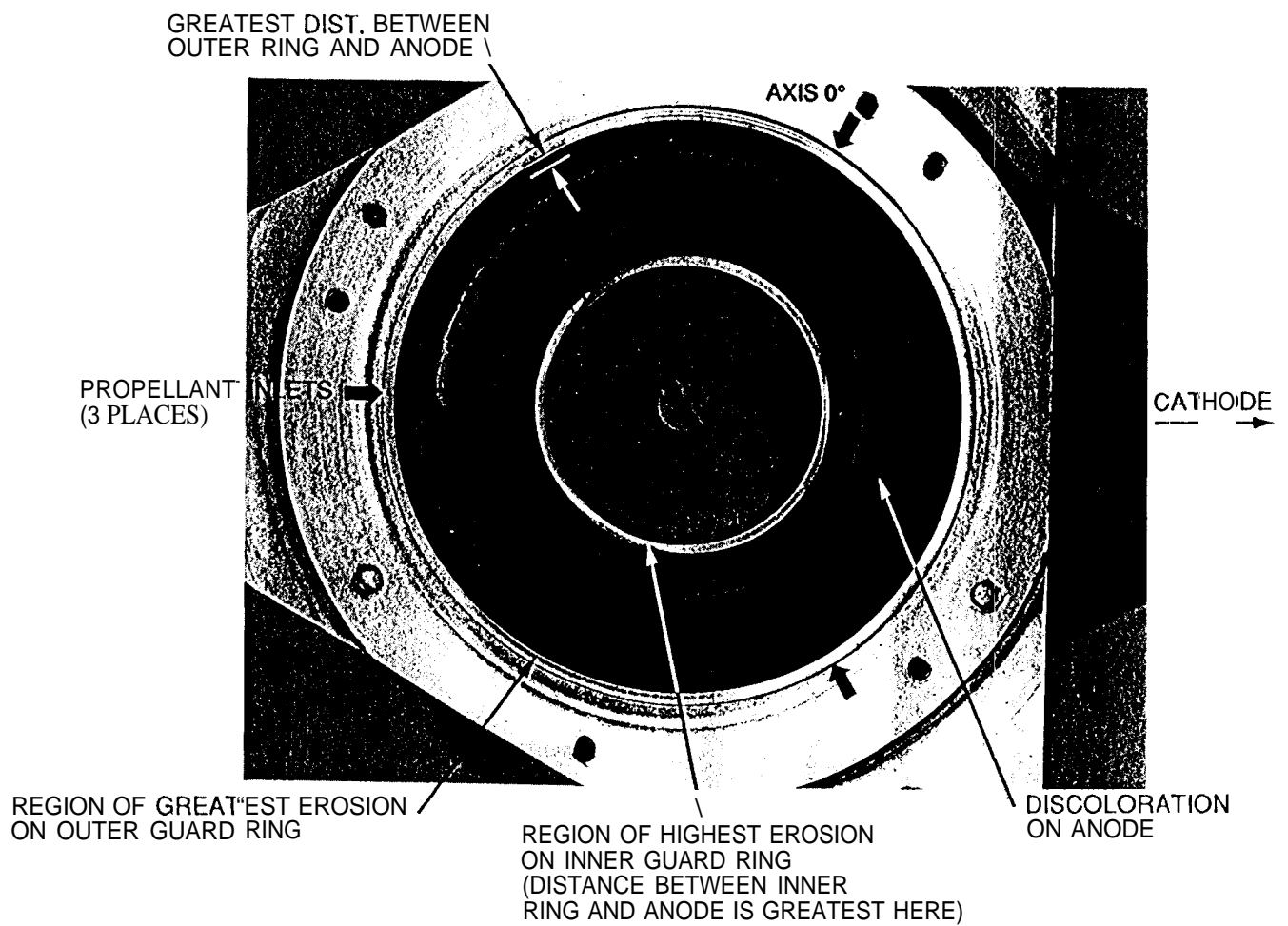


Fig. 7 Details of the D-55 erosion geometry.

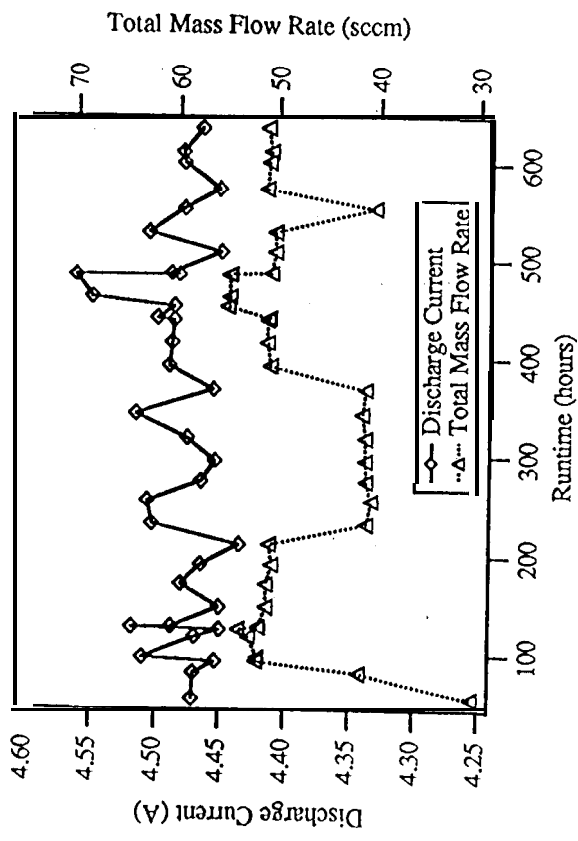


Fig 8(a). Discharge current and mass flow rate for wear test cycles 94-128.

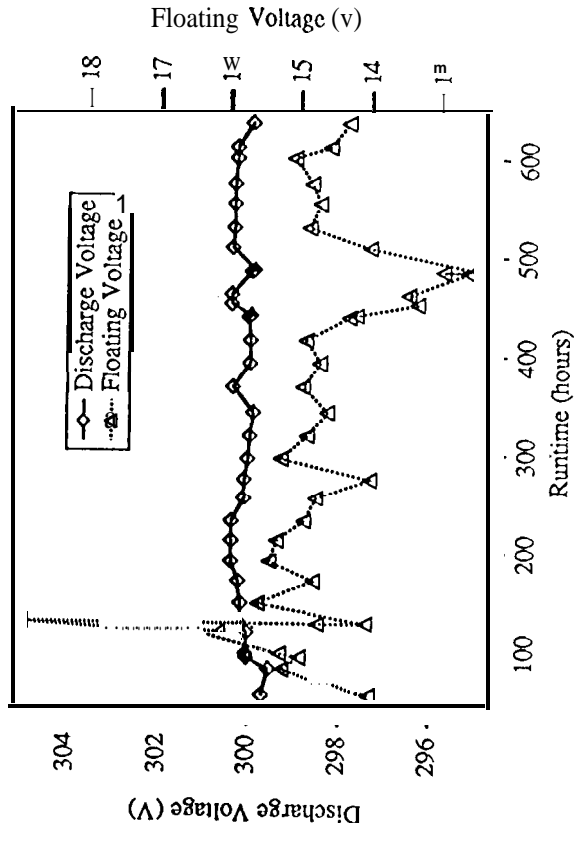


Fig. 8(b). Discharge voltage and floating voltage for wear test cycles 94- 28

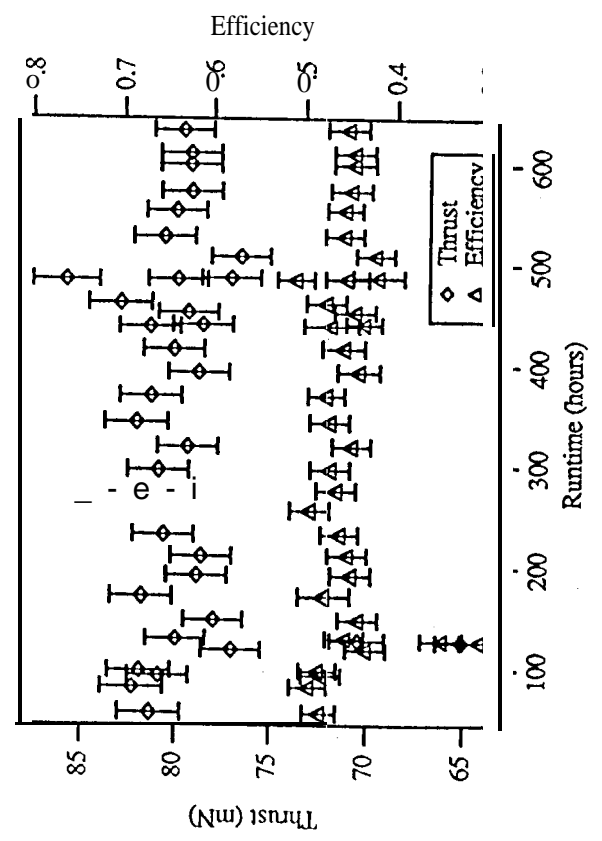


Fig. 8(c). Thrust and Efficiency for wear test cycles 94-128.

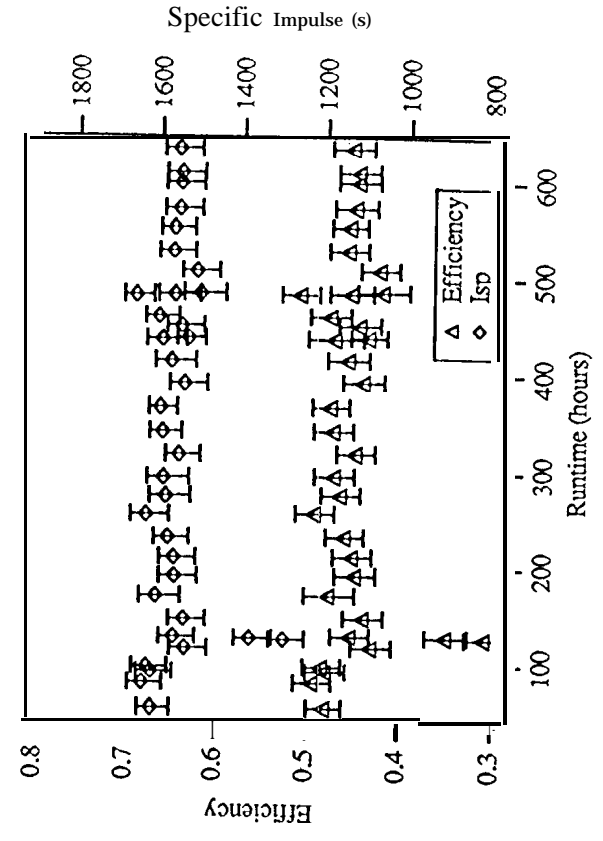


Fig. 8(d). Engine Efficiency and specific impulse for wear test cycles 94-128.

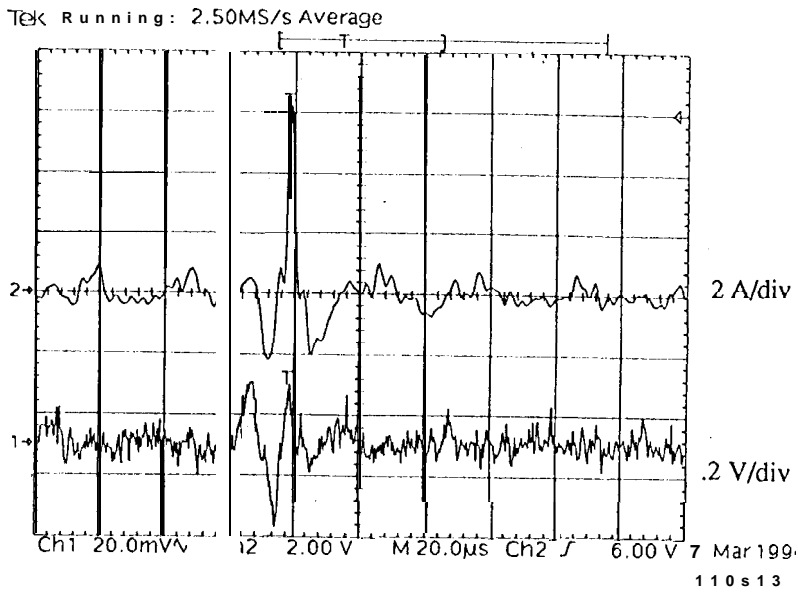


Fig. 9(a). Oscilloscope trace from cycle 95 taken just before engine shutdown.

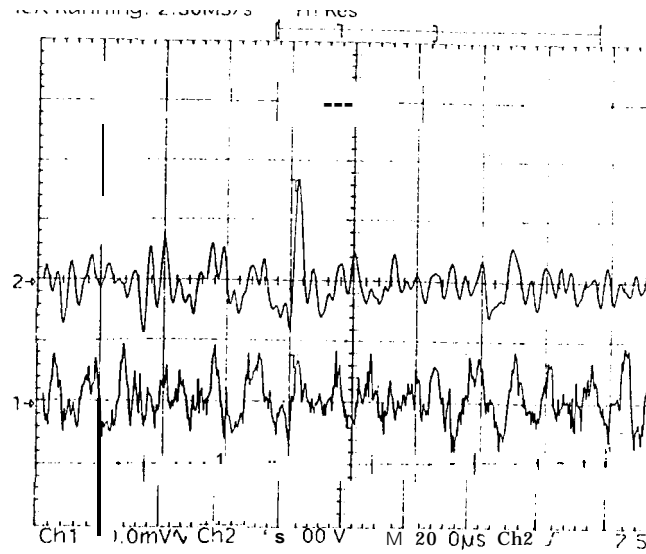


Fig. 9(b). Oscilloscope trace from cycle 126 taken just before engine shutdown.

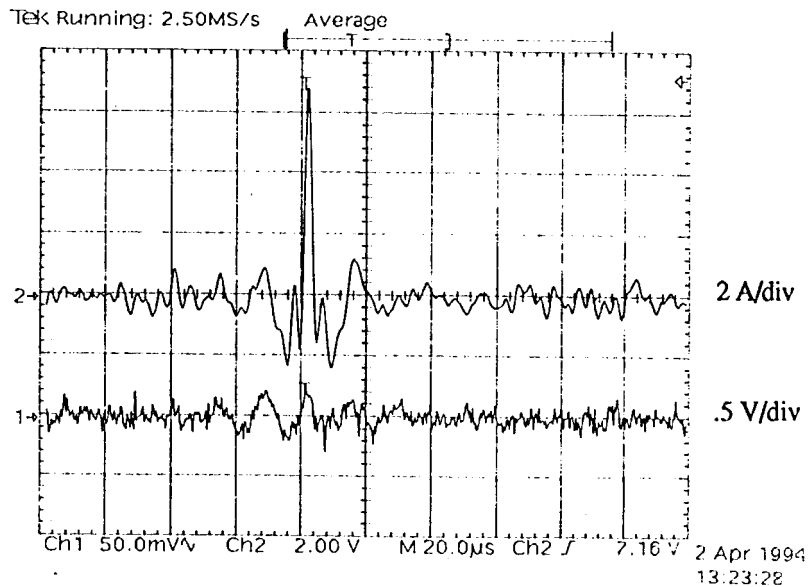


Fig. 9(c). Oscilloscope trace from cycle 126 taken just before engine shutdown,

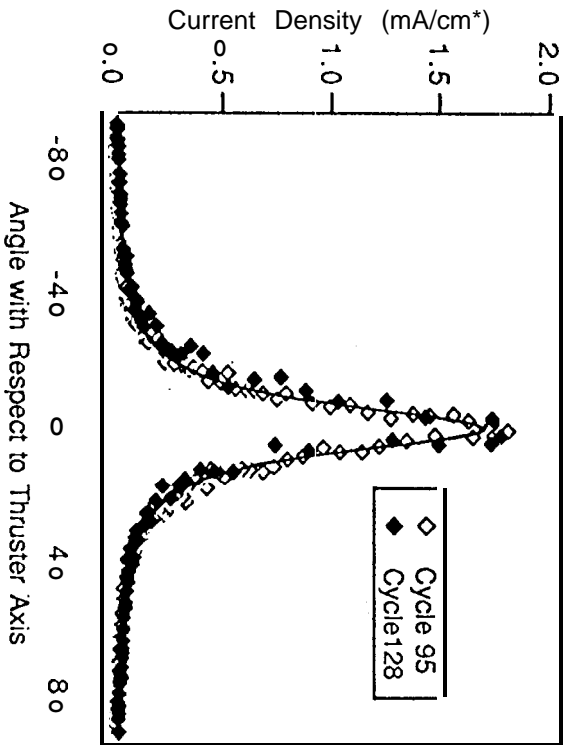


Fig. 10 Comparison of exhaust beam current density profile 1-m downstream of the thruster after 81 and 634 hours of operation

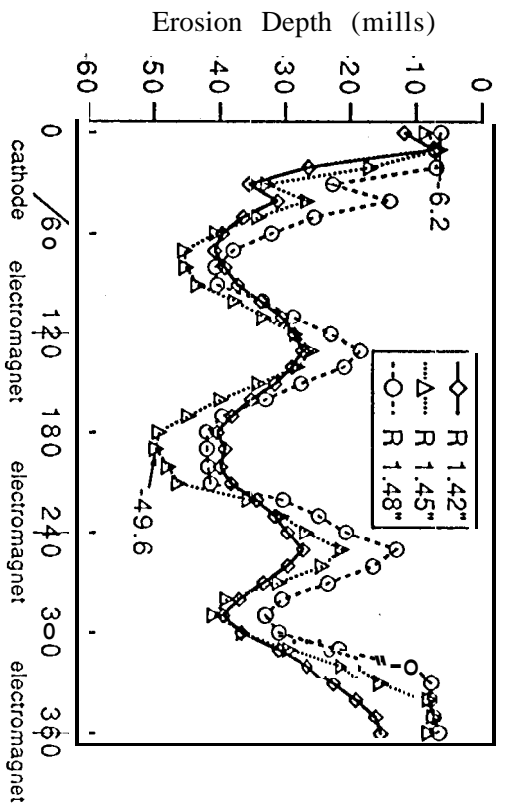


Fig. 11 Erosion depth measurements on the outer guard ring as a function of clock angle and radial distance.

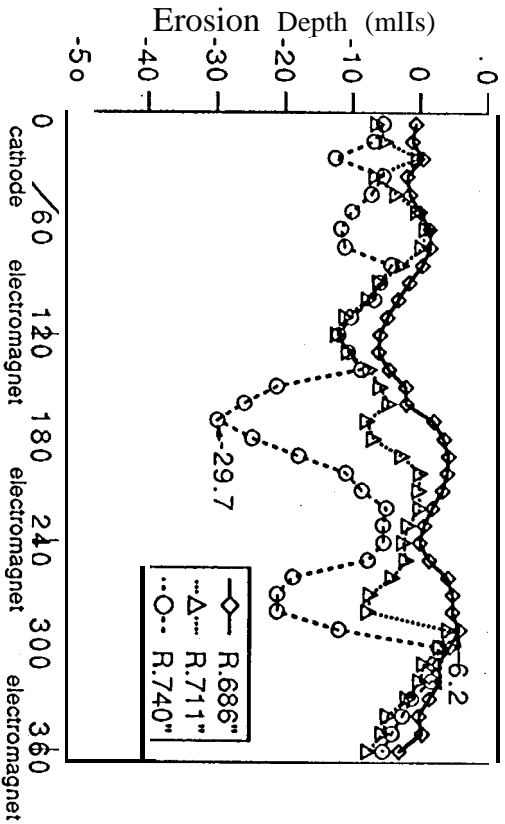


Fig. 12 Erosion depth measurements on the inner guard ring as a function of clock angle and radial distance.